JOURNAL OF Applied Polymer SCIENCE

Shape Memory Properties of Polycaprolactone-based Polyurethanes Prepared by Reactive Extrusion

Shengguang Weng, Zhean Xia, Jianding Chen, Luanluan Gong

Shanghai Key Laboratory of Advanced Polymeric Materials, Key Laboratory for Ultrafine Materials of Ministry of Education, School of Materials Science and Engineering, East China University of Science and Technology, Shanghai, People's Republic of China

Correspondence to: J. Chen (E-mail: jiandingchen@ecust.edu.cn)

ABSTRACT: The shape memory properties of polycaprolactone-based polyurethanes (PCLUs) synthesized via a novel route of reactive extrusion were investigated in terms of the deformation amplitude, temperature, and rate by differential scanning calorimetry (DSC), dynamic mechanical analyzer, and polarized optical microscopy (POM). DSC analysis shows that the crystalline melting temperature and crystallinity of PCLU increased monotonically with increasing the average polymerization degree ($\overline{DPn}$) of poly(ε-caprolactone) (PCL) block. The retract force increased with increasing the temperature and reached the maximum (6–7 MPa) within 45–55°C. Furthermore, a modified model with two recovery stages was postulated to elucidate the shape memory process, which is visually presented by POM analysis. The two stages of tensile and compressive recovery are distinguished by the inflexion temperature, within 43–48°C and 64–66°C, respectively. The shape fixity is about 60–70% and can be improved to 100% by choosing proper deformation temperature. The tensile deformation recovery ratio was 80–98% due to the water absorption, whereas the compressive deformation recovery ratio was almost 100%. Besides, recovery tests show that the lowest recovery temperature ranged from 24 to 47°C was influenced by the deformation temperature, rate and the PCL block ($\overline{DPn}$). Thus, the shape memory properties can be adjusted according to different purposes. © 2012 Wiley Periodicals, Inc. J. Appl. Polym. Sci. 000: 000–000, 2012

KEYWORDS: block copolymers; polyurethanes; reactive extrusion; structure–property relations

Received 8 January 2010; accepted 20 March 2012; published online
DOI: 10.1002/app.37768

INTRODUCTION

Shape memory polymers, as novel smart materials, have attracted extensive interest[1–16] for their potential promising applications including biomaterials,[1,17] actuators,[5] sensors,[18] and smart textile.[19] In general, the shape memory effect was realized by the cooperation of the chemical or physical cross links and the reversible network chains, which can play the roles of fixed phase and molecular switch,[4,12,16] respectively. The cross links are employed in the course of shape memorization to memorize the original shape. Although the reversible network chains are designed to have a thermal transition at certain temperature, which can be either T_g (the reversible network chains are amorphous) or T_m (the reversible network chains are crystalline). The reversible network chains are flexible, and therefore the polymers can develop large deformation above the transition temperature. In contrast, they are frozen to lose mobility, and thus the polymers can fixed in a temporary shape below the transition temperature.

Shape memory polyurethanes have been an important category in the shape memory polymer family because certain segmented polyurethanes were found to exhibit shape memory effect.[14,15,17] Due to the thermodynamical dissimilarity, the shape memory polyurethanes will separate into hard-segment and soft-segment microphases, which play the roles of fixed phase and reversible network chains for the shape memory effect, respectively.[4,16] Many attempts have been made to elucidate the relationship between the structure and shape memory effect of the polyurethanes.[14,15,20–25] The morphology of phase separation, phase composition, microdomain sizes, phase distribution, and so on were investigated to optimize the molecular design and explore applications of shape memory polyurethanes. A series of shape memory polyurethanes having crystalline reversible phase were also studied to understand the effects of soft-segment length and hard-segment content on shape memory properties.[5,26–28] Nevertheless, the relationship between morphological structures and shape memory properties is quite complicated and still under detailed investigations. In contrast, the thermomechanical

conditions, especially the deformation amplitude, temperature and rate, could exert significant influence on the shape memory behaviors.[29–33] This means the thermomechanical conditions would affect the shape memory polyurethanes with different structures in different manners and degrees. This has not been reported in detail yet. In addition, as far as we know, almost all the reported shape memory polyurethanes were obtained from the flask via several separated steps in a small scale.

In this article, we report the polycaprolactone-based polyurethane (PCLU) synthesized via a novel route of reactive extrusion in a mass scale. Compared with the reported fabrication of PCLU, the *in situ* reactive extrusion preparation not only explored a convenient, effective approach for fabrication of PCLU but also offer a simplified controllable approach for the production of PCLU in a successive mass scale. The shape memory properties (temporary shape fixity and shape recovery ratio) of PCLUs were investigated. The thermal behaviors and the crystal microdomains morphology associated with shape memory properties were studied with the combination of multiple techniques. The effects of different thermomechanical conditions in terms of the deformation amplitude, temperature and rate on the shape memory properties were investigated to optimize the shape memory properties according to different purposes. Different deformation temperatures, especially lower than the crystalline melting temperature (T_m), were adopted to obtain an enhanced retract force and explore the effect of the deformation of crystal microdomains on the shape memory properties. Furthermore, a modified model was postulated for the description of the shape memorization process. It was verified to be quite good for the model to elucidate the development of retract force and recovery of dimensions.

EXPERIMENTAL

Materials

ε-Caprolactone (CL) (from Solvey), polyethylene glycol (PEG400, PEG1000, and PEG4000; M_W = 400, 1000, and 4000 g/mol, respectively, functionality = 2) and poly(tetramethylene oxide) glycol (PTMG-1000; M_W = 1000 g/mol, functionality=2) were purified by vacuumed distillation at 100°C to remove absorbed water. 4,4′-Diphenylmethane diisocyanate (MDI; from Wanhua Corp.) and titanium propoxide $Ti(OPr)_4$ (from Aldrich) were used as received.

Preparation of PCLU Samples

PCLU samples used in this study were obtained from polyether diol (PTMG or PEG) according to our previous work[34] by reactive extrusion in the corotating twin screw extruder of which the barrel temperature profile between the hopper and the die was 190°C, and the rotating rate was 100 r/min. A typical experimental procedure was as follows: a calculated amount of $Ti(OPr)_4$ mixture modified by polyether diol and MDI were dissolved in CL monomer to make the "Solution A" and "Solution B," respectively. Solutions A and B were pumped individually into the barrel by two pumps. The flow rates were controlled and monitored to ensure that the stoichiometric ratio of hydroxyl group to isocyanate group was 1 : 1 and the total flow rate of Solutions A and B was 5 kg/h. The PCLU product was extruded out of the die, cooled with cold water, dried by blast and cut into pellets. According to different polyether diols from which PCLUs originated, different PCLU pellets were obtained, PTMG1000-DPn25, PTMG1000-DPn30, PTMG1000-DPn35, PTMG1000-DPn40, PEG1000-DPn20, PEG1000-DPn25, PEG1000-DPn30, PEG1000-DPn35, PEG1000-DPn40, PEG400-DPn20, PEG400-DPn25, PEG400-DPn30, PEG400-DPn35, PEG400-DPn40, PEG4000-DPn12, PEG4000-DPn21, and PEG4000-DPn25. The reaction mechanism, monomer conversion, molecular weight, and structure were reported in another article[34].

Differential Scanning Calorimetry

Differential scanning calorimetry (DSC) was carried out on a TA MDSC 2910 over a temperature range from −40°C to 200°C and with a heating rate of 10°C/min. The sample was heated to 200°C, then cooled to −40°C and heated to 200°C. The peak temperatures of the melting peak and crystallization peak were taken as the crystalline melting and crystallization temperatures (T_m and T_c) of the sample, respectively, which are given in Table I. The crystallinity was calculated according to eq. (1) from the melting enthalpy data ΔH_c of the crystallization peak by using the 0.14 J/kg enthalpy value for fusion of 100% crystalline poly(ε-caprolactone) (PCL) given by Crescenzi et al.[35]

$$X_c = \frac{\Delta H_c}{\Delta H_{100} \cdot \omega_{CL}} \times 100\% \quad (1)$$

where ΔH_c and ΔH_{100} are the melting enthalpy of the sample and 100% crystalline PCL, respectively; ω_{CL} represents the mass fraction of PCL block in the PCLU.

Water Absorption

The water absorption measurements of the samples were carried out in a water bath where the temperature can be adjusted and controlled at fixed constant temperature. A rectangular sample bar, size of 25 mm × 7 mm × 3 mm, was dried in a vacuumed oven at 30°C over night before test. The precise dimensions and weight of the sample were recorded every 10 min after it was immersed into the water bath. The test was continued until the equilibrium weight reached. The water absorption (Wa) of the sample was calculated according to eq. (2)

$$\text{Wa}\% = \frac{m_t - m_0}{m_0} \times 100\% \quad (2)$$

where m_0 and m_t denote the weights of the sample before immersing into the water and after immersing for time t, respectively.

Polarized Optical Microscopy

A 0.5-mm-thick PCLU film used for polarized optical microscopy (POM) measurement was prepared by casting a 5-wt % chloroform solution of the copolymers on a polytetrafluorethylene mold and then airing for 2 days at room temperature followed by drying under vacuum for 2 days. The morphology of crystal microdomains was observed under a POM (Nikon Eclipse LV100POL) equipped with crossed polarizers.

Shape Memory Properties

Tensile Deformation Recovery Test. The PCLU pellets obtained by reactive extrusion were mold pressed at 160°C into

Table I. DSC Data for PCLUs in Different Heating and Cooling Runs

	First heating run			Cooling run			Second heating run		
Samples	T_{m1} (°C)	ΔH_{m1} (J/g)	PCL X_c (%)	T_c (°C)	ΔH_c (J/g)	PCL X_c (%)	T_{m2} (°C)	ΔH_{m2} (J/g)	PCL X_c (%)
PTMG1000-DPn25	56.3	51.36	52.8	16.3	39.35	40.4	46.0	39.37	40.4
PTMG1000-DPn30	58.8	70.31	68.6	21.1	49.42	48.2	48.5	49.63	48.4
PTMG1000-DPn35	58.2	61.06	57.3	19.4	46.03	43.2	48.8	47.32	44.4
PTMG1000-DPn40	57.7	64.84	59.0	20.5	46.30	42.1	49.9	46.16	42.0
PEG1000-DPn20	52.7	56.96	63.0	24.4	37.04	40.9	48.4	39.36	43.5
PEG1000-DPn25	56.2	59.46	61.1	23.7	38.94	40.0	48.2	43.82	45.0
PEG1000-DPn30	55.7	68.70	67.0	24.6	50.41	49.2	51.1	52.77	51. 5
PEG1000-DPn35	55.5	70.16	65.8	25.4	51.79	48.6	51.3	53.97	50.6
PEG1000-DPn40	54.8	69.83	63.5	27.3	51.84	47.2	51.9	53.94	49.1
PEG400-DPn20	52.2	69.52	63.8	21.0	45.78	42.0	45.3	50.26	46.1
PEG400-DPn25	55.0	71.19	62.4	23.3	49.45	43.4	47.2	52.52	46.1
PEG400-DPn30	56.5	73.71	62.6	23.8	52.59	44.7	48.4	54.49	46.3
PEG400-DPn35	57.8	73.93	61.4	22.9	52.16	43.3	49.6	56.14	46.6
PEG400-DPn40	57.8	80.46	65.7	24.8	52.26	42.6	50.1	57.07	46.6
Pure PCL	63.6	97.41	69.6	30.3	66.41	47.4	54.9	72.21	51.6

a 3-mm-thick PCLU plate and cooled to room temperature within 10 min with a pressure of 10 MPa. Dumbbell-shaped specimens (effective dimension: 30 mm long × 4 mm wide × 3 mm thick) were cut from the plates. The tensile tests were performed on a new SANS CMT6104 electron tester. For the tensile shape memory measurement, typically, a specimen was elongated at a drawing rate of 50 mm/min or 100 mm/min at room temperature until the elongation of 200% or 300% reached. After the specimen was released, it was clamped again. The elongated specimen with fixed length was placed at room temperature for more than a week to develop the crystallization fully. To measure the retract force, one specimen was heated at a rate of 10°C/min until 70°C, and the tensile stress was recorded as a function of the temperature. For the measurement of recovery of elongated length, a water bath was used to get different constant temperatures, the temperature of which was elevated from 20°C to 60°C with increment of 1°C. After each temperature of the water bath was kept constant for 5 min, a specimen was immersed into the water bath for 5 min and the length was recorded as a function of the recovery temperature. The temporary shape fixity R_f and the shape recovery ratio R_r of the tensile deformation recovery cycle were calculated with the following equations:

$$R_f = \frac{\varepsilon_u}{\varepsilon_m} \times 100\% \quad (3)$$

$$R_r = \frac{\varepsilon_m - \varepsilon_p}{\varepsilon_m} \times 100\% \quad (4)$$

where ε_m denotes the maximum strain in the tensile test; ε_u is the residual strain after unloading at room temperature, and ε_p is the residual strain after shape recovery.

Compressive Deformation Recovery Test. A cylinder of φ = 10 mm cut from a 3-mm-thick PCLU plate was compressed into a 2-mm-thick disk at different temperatures, ranged from 25°C to 55°C, kept at room temperature for 10 min, and then cut into φ = 5 mm disk at room temperature for dynamic mechanical analyzer (DMA) measurement. The deformed specimen was placed at room temperature for more than a week before test. The temporary shape fixity R_f' was calculated according to eq. (5). The thermomechanical analysis was conducted on a TA DMA 2980 in the temperature range from 10°C to 70°C at a heating rate of 5°C/min by penetration mode with a controlled force of 0.005 N. The thickness of disk was recorded as a function of temperature. The shape recovery ratio R_r' was calculated according to eq. (6) by the thickness before and after a compressive deformation recovery cycle.

$$R_f' = \frac{\varepsilon_u'}{\varepsilon_m'} \times 100\% \quad (5)$$

$$R_r' = \frac{\varepsilon_m' - \varepsilon_p'}{\varepsilon_m'} \times 100\% \quad (6)$$

where ε_m' denotes the maximum strain in the compressive test; ε_u' is the residual strain after unloading at room temperature; and ε_p' is the residual strain after shape recovery.

RESULTS AND DISCUSSION

Thermal Properties of PCLU

The crystalline melting and crystallization behaviors of PTMG–PCLU and PEG–PCLU were investigated by DSC. DSC results for PCLUs of the first heating, cooling, and second heating runs were summarized in Table I. It shows that all the products were crystalline. The T_c, T_m, and X_c of PCLUs are all dependent on the PCL block ($\overline{DPn}$) and the molecular weight of the polyether diol blocked in the PCL chains. In general, they all have a monomodal endothermic peak of the melting of PCL block crystal in the first and second heating run. Because the polyether (PEG or PTMG) diol has been converted to be PCL–PEG–PCL or PCL–PTMG–PCL copolymer diol, the PCL block

Applied Polymer SCIENCE

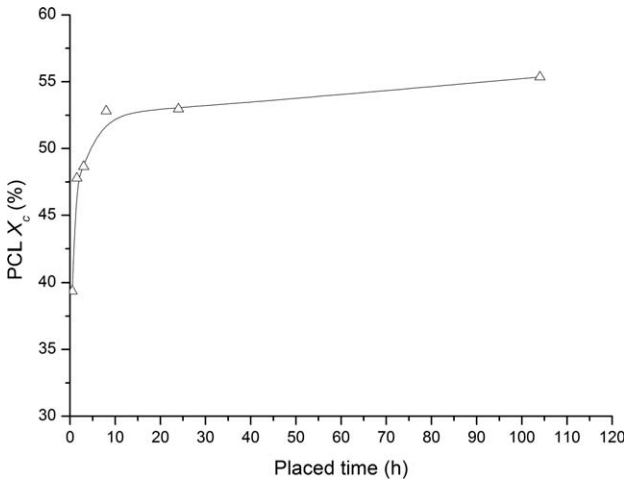

Figure 1. The crystallinity of PEG400-DPn30 of different times placed at room temperature.

can still crystallize and lead to less perfect crystal due to the restriction effect of polyether block. On the contrary, the crystallization of the polyether block was also restricted by the PCL block and did not crystallize at all when PCL block ($\overline{DPn}$) was more than 20.[36–38] Therefore, there is only one crystalline melting peak in the DSC curve and the melting peak of polyether block disappeared in the discussed range of the PCL block ($\overline{DPn}$), from 20 to 40. The X_c and T_c show slight dependence on the PCL block ($\overline{DPn}$), which results partly from their similar crystallinity to that of pure PCL. Nevertheless, the T_m of the products almost increased with increasing the PCL block ($\overline{DPn}$), which indicates that the crystal of PCL block tends to be more perfect with the increase of PCL block ($\overline{DPn}$) according to Flory's elucidation.[39] Furthermore, the T_m and melting enthalpy of the first run are more than those of the second heating run. More detailed, there is a difference of 7–10°C in T_m and 11–19 J/g in melting enthalpy for the PTMG–PCLU, and 2–8°C and 14–20 J/m for PEG–PCLU, respectively. The difference indicates that the PCL block crystallization will still develop at room temperature after nonisothermal crystallization during the cooling run.

Although the PCL block in PCLUs is crystalline, the T_m and melting enthalpy of PTMG–PCLU and PEG–PCLU are lower than those of pure PCL of the same molecular weight (54.91°C and 72.21 J/g, respectively). The difference between the crystalline melting of PCLU and pure PCL results from two can be ascribed into the following two reasons. In contrast, the molecular weight of the PCL block in the copolymer is much lower than that of pure PCL, which leads to less perfect crystals during the crystallization of the PCLU copolymer.[39] In contrast, the polyether molecular chain blocked in the copolymer restricted the crystallization of PCL chain, which also resulted in less perfect crystals of the PCL block. However, the effect of restriction on the crystallization of the PCL block decreased with the increase of the PCL block ($\overline{DPn}$). It is favorable that the T_m can be adjusted by setting the PCL block ($\overline{DPn}$) and introducing the polyether chain segment into the molecular chain.

To investigate the effect of the placed time (the time for the sample to be placed at room temperature from the moment that the sample was extruded from the die of the twin screw extruder) on the crystallinity of PCLU, the crystallinity of PEG400-PCLU with the PCL block ($\overline{DPn}$) of 30 was measured at different placed times at room temperature. Figure 1 plots the crystallinity of PEG400-DPn30 against different placed times from the moment it was fabricated via reactive extrusion. When placed at room temperature for 0.5–1 h, the crystallization of the product only developed to 60–70% of the ultimate crystallinity of placed for more than 7 days. Although the crystallinity at placed time of 8 h has reached about 90% of the ultimate crystallinity, the T_m was still much lower than that of the ultimate product (as shown in Figure 2). Moreover, there is a melting region at the temperature range of 20–30°C, which is much lower than the crystalline melting point and shifts to high temperature region with the increase of placed time. It implies that the less perfect crystal developed when placed at room temperature and the crystal turned gradually to be more perfect with increasing the placed time. This portion of less perfect crystal also broadened the crystalline melting peak of the ultimate product to some extent. Thus, to achieve good shape memory properties, the shape recovery test should be performed after the deformed specimens have been placed for more 7 days to develop their crystallization fully.

The Retract Force of PCLU

Figure 3(a–d) shows the retract forces of PTMG1000-PCLU elongated to 200% and 300% at different drawing rates, respectively, as a function of the temperature raised at a rate of 10°C/min. The retract force of PCLU is determined by the cross links set by the crystal microdomains of PCL block and by the polyurethane microphase separation. As the temperature was elevated, the retract force increased to its maximum in the temperature range of 45–55°C before the crystalline melting of PCL block and then turned to decrease with the T_m of PCL block crystal approached. Nevertheless, it was found that the temperature corresponding to the maximum retract force (T_{Fmax}) was much lower than the T_m of PCL block crystal. Above the T_{Fmax} of the specimen, as all crystal of PCL block were melted

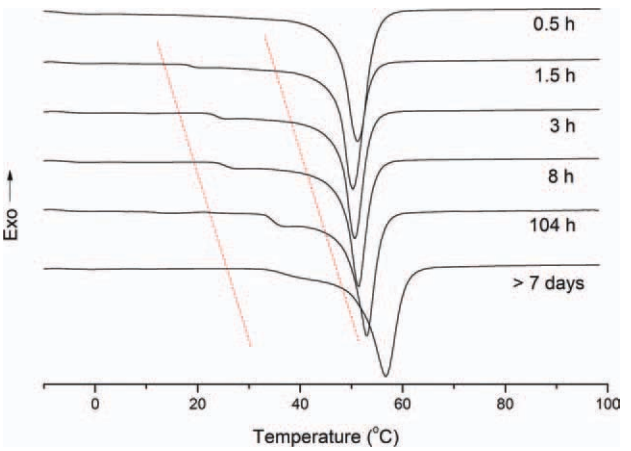

Figure 2. DSC curves of PEG400-DPn30 of different times placed at room temperature. [Color figure can be viewed in the online issue, which is available at wileyonlinelibrary.com.]

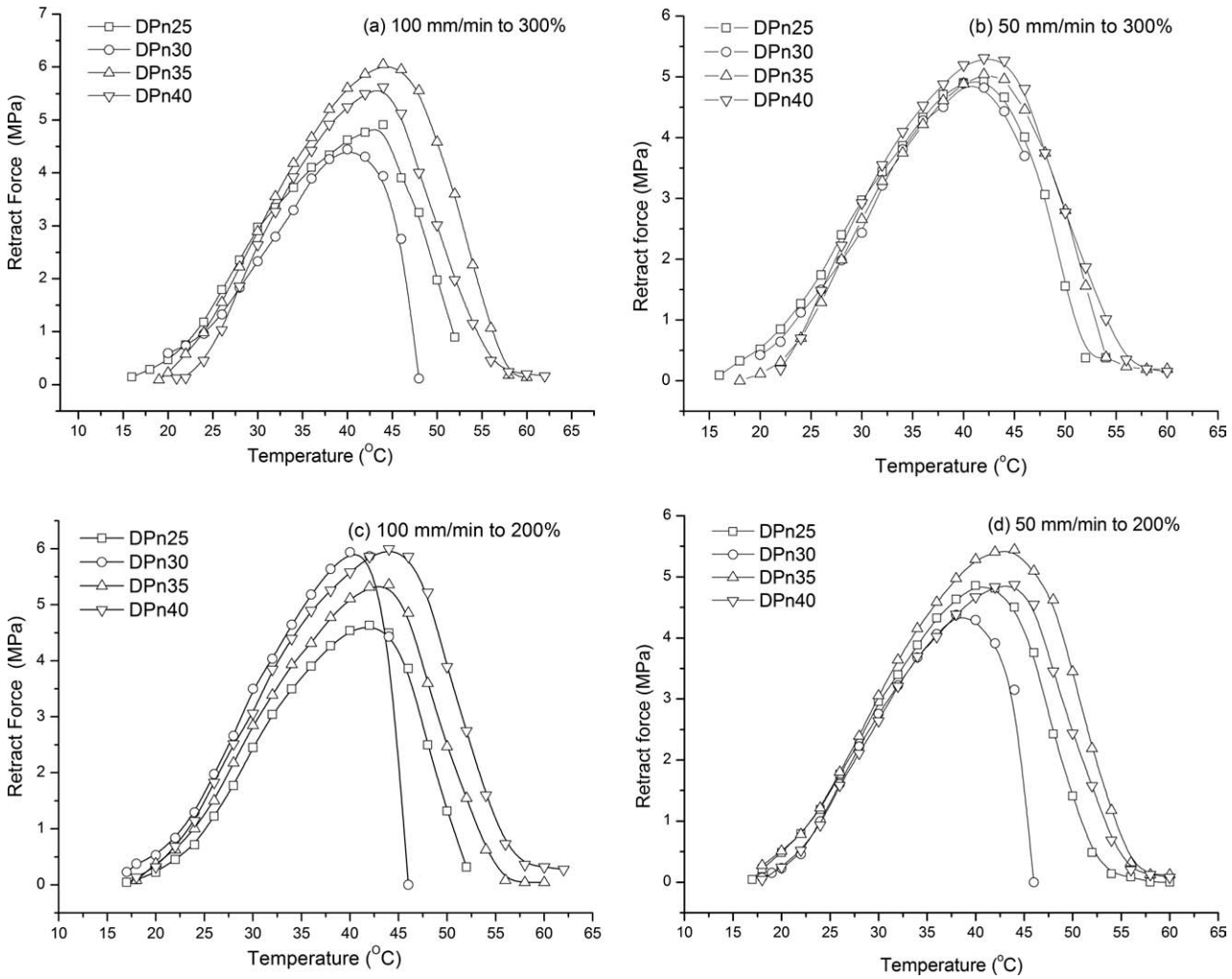

Figure 3. Retract force curves of PTMG1000-PCLU.

gradually and the cross links set by PCL block crystal microdomains was dissociated, the retract force decreased gradually due to the relaxation of PCLU molecular chain and finally reduce to a very low level with which can only sustain the specimen not to be broken. It implies that the most perfect crystal microdomains and microphase separation together form the drive force for the shape recovery below the T_m of PCL block crystal, whereas above T_m the cross links set by the microphase separation drives the recovery to the original shape.

Furthermore, the drawing rate, or deformation rate, will evidently affect the maximum retract force and the development of retract force. For the specimens elongated at a drawing rate of 100 mm/min, the development of retract force can clearly distinguish the PCLUs of different PCL block $\overline{DPn}$ s. The maximum retract force varied from 4.4 MPa to 6.2 MPa. Although for the specimens elongated with a rate of 50 mm/min, the difference among PCLU of different PCL block $\overline{DPn}$ s turns to be slight, which varied from 4.3 MPa to 5.2 MPa. When deformed at a higher rate, for example 100 mm/min in tensile elongation, the crystal microdomains were deformed less for they cannot keep up with the elongation of the specimen. And the destructive deformation of crystal microdomains was less, that is, the PCL block crystal can maintain its perfectness to a great extent. Therefore, the retract force determined by the deformed crystal microdomains can develop to a high level and its maximum value will reach at a higher temperature and vice versa. In addition, both the maximum retract force and T_{Fmax} are dependent on the PCL block $\overline{DPn}$. It is reasonable that increasing the PCL block $\overline{DPn}$ will obviously lead to higher crystallinity and more perfect crystal of PCL block, which ensures the crystal microdomains to develop a lower deformation when elongated.

The lowest recovery temperature also increased with the increase of the PCL block $\overline{DPn}$ and the deformation rate. This can be explained by the perfectness degree of PCL block crystal and the deformation degree, as discussed above. The retract force developments of PEG400-PCLU and PEG1000-PCLU are similar to that of PTMG1000-PCLU and typical curves were plotted in Figures 4–6. It is worth noting that the maximum retract force values of the PCLUs (6–7 MPa) are as high as those for polylactic acid-based polyurethanes (PLAUs; about 7

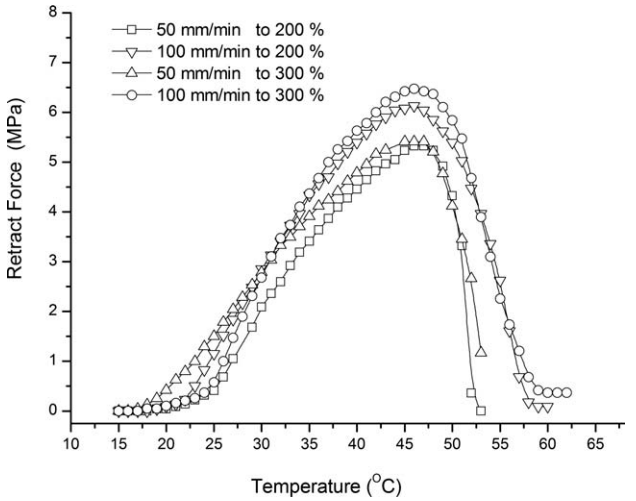

Figure 4. Typical retract force curves of PEG400-PCLU of PCL block $\overline{DPn}$ 30.

MPa).[40,41] This means that the shape recovery of PCLUs can be as rapid as that of PLAUs by choosing proper deformation conditions.

As for the polyether molecular chain length, the molecular weight increased from 400 to 1000, it did not affect the retract force greatly. However, when increased to 4000, it does affect the retract force greatly as shown in Figure 6(a,b). In contrast to the PCLUs discussed above, the PCLU blocked with PEG of molecular weight 4000 has a much lower retract force than that of PEG400, PEG1000, and PTMG-1000, 1.2 MPa vs approximate 6–7 MPa. And the T_{Fmax} of the PEG4000-PCLU are also much lower. It results from the restriction effect of polyether block PEG4000 on the crystallization of PCL block. However, the PEG4000 can also crystallize during the crystallization of PCL block and its crystal microdomains was deformed and interacted with PCL block crystal microdomains when deformed. The efforts to understand the mechanism of interaction between the two crystal microdomains are still proceeding by our group.

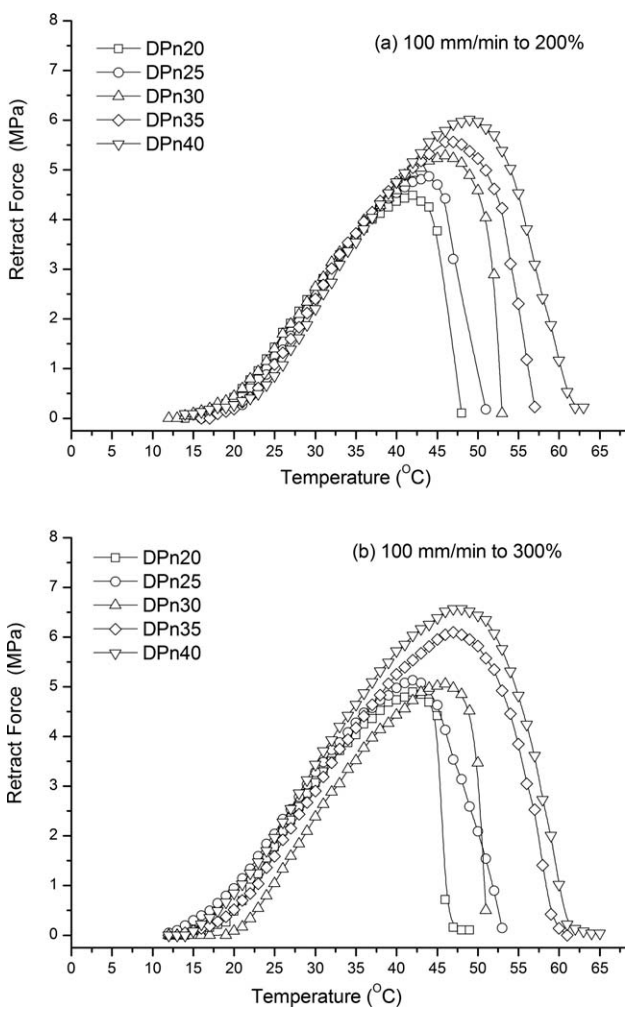

Figure 5. Retract force curves of PEG1000-PCLU with different PCL block $\overline{DPn}$.

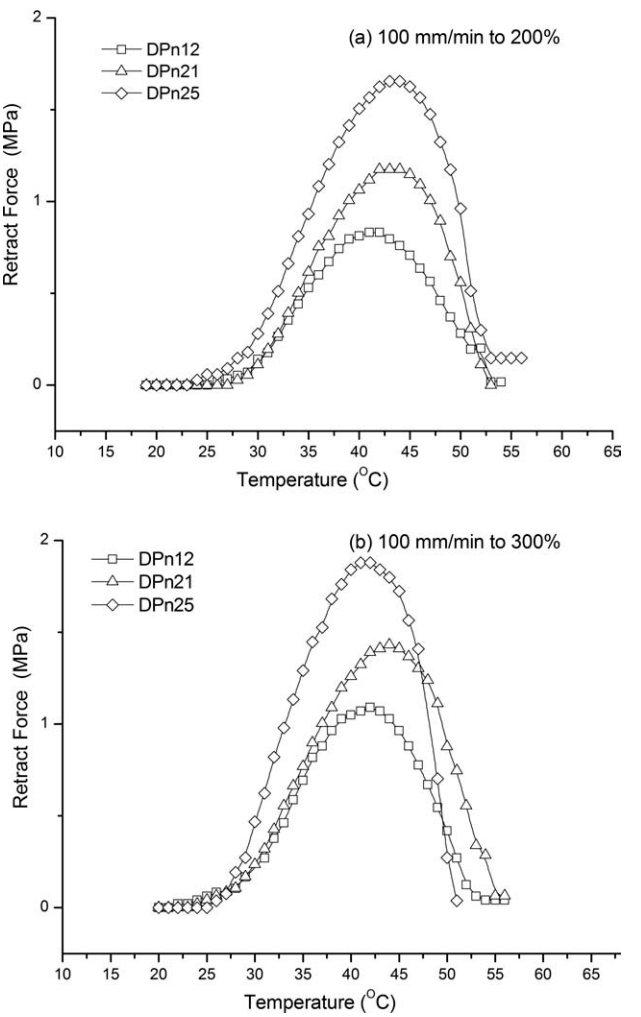

Figure 6. Retract force curves of PEG4000-PCLU with different PCL block $\overline{DPn}$.

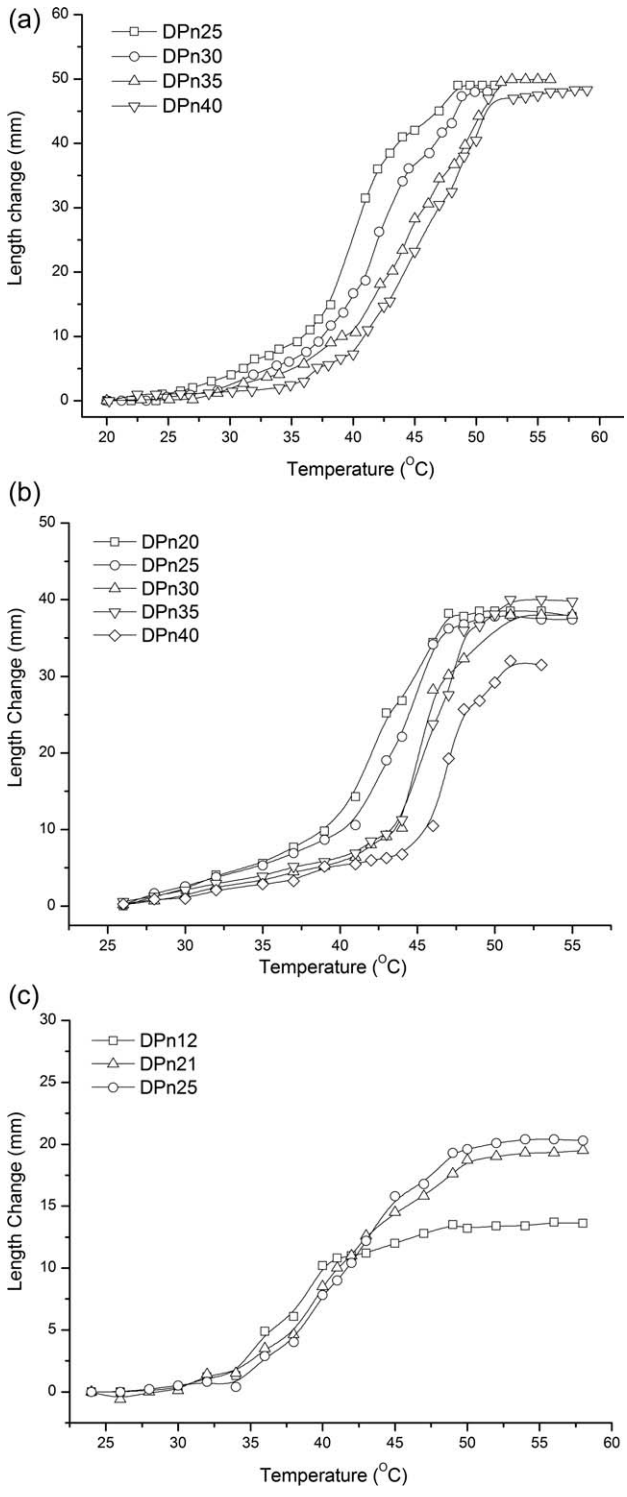

Figure 7. Tensile deformation recovery curves of (a) PTMG1000-PCLU, (b) PEG1000-PCLU, and (c) PEG4000-PCLU elongated at 100 mm/min to 300%

The Recovery of Tensile Deformation

A unique feature of shape memory polymers induced by heating is the ability to recover their original shape on heating to the transition temperature (T_g or T_m). In our work, the recovery of original shape is switched by the T_m of PCL block. The recovery curves of 300% elongation for PCLU specimens originated from different polyether diols are given in Figure 7(a–c), respectively. And the data from recovery curves, including 200% and 300% elongation, are summarized in Table II. Results show that the influence of PCL block $\overline{DPn}$ on the tensile deformation recovery properties is similar for PCLUs originated from different polyether diols. Roughly, the LRT and the upper recovery temperature (URT) increased with the increase of the PCL block $\overline{DPn}$.

Furthermore, it is apparent that there were two stages in the recovery process, which were distinguished by an inflexion temperature. Take the recovery of PTMG1000-PCLU specimen as an example, the inflexion temperature increased with the increase of the PCL block $\overline{DPn}$, approximately 43–48°C. The inflexion temperature is lower than the T_m of the corresponding product by 8–10°C. Interestingly, the inflexion temperature is almost equal to the temperature at which the maximum retract force reached. The two stages of recovery driven by different drive forces were also verified by the recovery process of tensile deformation, which were distinguished more clearly by the inflexion temperature. Below the inflexion temperature, the recovery was driven by the recovery of deformed crystal microdomains as well as the cross links set by the most perfect crystal and polyurethane microphase separation. The deformed PCL crystal microdomains were strongly inclined to restore their original shape, which reflected in the curve as a steeper recovery. With the inflexion temperature approached, the deformed crystal microdomains recovered almost completely and the crystallinity of the specimen decreased to such a slim content that the crystal microdomains cannot act as cross links. Herein, the recovery was in the second stage where the recovery was driven alone by the cross links set by polyurethane microphase separation and the retract force was lowered greatly.

Table II. Tensile Deformation Recovery Results for PCLU with Different Polyether Diols and $\overline{DPn}$ s

	100 mm/min to 200%		100 mm/min to 300%	
Sample no.	R_f (%)	R_r (%)	R_f (%)	R_r (%)
PTMG1000-DPn25	87.0	88.4	86.5	87.3
PTMG1000-DPn30	74.0	91.0	73.3	88.7
PTMG1000-DPn35	70.8	100	70.4	98.8
PTMG1000-DPn40	66.5	100	71.1	98.7
PEG1000-DPn20	54.2	84.6	73.1	78.3
PEG1000-DPn25	61.2	82.0	69.6	80.7
PEG1000-DPn30	79.2	77.0	77.3	82.9
PEG1000-DPn35	77.2	67.3	77.2	75.2
PEG1000-DPn40	66.2	73.0	64.3	78.0
PEG400-DPn20	67.9	91.7	68.8	90.6
PEG400-DPn25	70.9	93.7	69.7	93.0
PEG400-DPn30	70.6	92.7	70.1	92.2
PEG400-DPn35	70.7	95.7	70.3	94.1
PEG400-DPn40	70.4	96.6	70.2	94.8

More detailed, as shown in Table II, the shape fixity R_f of products is around 60–70%, and the differences of R_f among various products with different PCL block $\overline{DPn}$ are not significant. In our work, the tensile test and the temporary shape fix test were both performed at room temperature. That is, the PCL block crystal was not melted when the specimens were stretched. Thus, the elongation of the specimens must be accompanied by the deformation of the PCL crystal microdomains as well as the destruction of part of PCL crystal. The destructed part of PCL crystal microdomains turned to be amorphous region which resulted in the elasticity of the specimen, whereas the deformed part fixed the temporary shape of the specimen. In addition, the polyether (PTMG or PEG) molecular chain blocked in the two PCL blocks was restrained in amorphous state due to the nature of competitive crystallization between PCL and polyether block molecular chains. The parts in amorphous state depressed the R_f of the specimen. The more PCL crystal microdomains were destructed into amorphous parts, the lower shape fixity resulted in. As for the effect of PCL block $\overline{DPn}$ on the R_f, however, no systematic variation is observed in our work, which partially results from the erratic variation of crystallinity of the products in the first heating run shown in Table I. The R_r is anticipated to increase with increasing the PCL block $\overline{DPn}$. Because the perfectness degree of the PCL crystal increased with the increase of the PCL block $\overline{DPn}$, the recovery effect resulted from the deformed crystal microdomains increased gradually. But for the PEG1000-PCLU, it is not the case owing to the strong water absorption of PEG1000 polyether.

The effect of prefixed elongation on R_f and R_r of the products was also investigated. Roughly, the R_f and R_r of 200% prefixed elongation are more than those of 300%, although the differences are quite small (as shown in Table II). This can be explained by that the higher elongation developed, the more elasticity resulted from more destructed PCL crystal. The more destructed PCL crystal means that more molecular chains turned into amorphous state, which resulted in more elasticity in the specimen. The elasticity is unfavorable to the shape fixation. In contrast, the more portion of PCL crystal was destructed, the less deformed crystal microdomains were available for shape fixity and recovery. Therefore, both R_f and R_r decrease with increasing prefixed elongation.

It should be noted that the recovery of tensile deformation tests were performed in the water to obtain a stable temperature environment. The water absorbed by the product will swell the specimen and greatly affect the dimensional recovery and stability. To investigate the effect of water absorption on the shape recovery, the water absorption of different products and its effect on the dimensional stability were studied. Results show that the water absorption ratio in weight is 1.9–2.2% for PTMG1000-PCLU in 25°C water bath, 15.0–24.9% for PEG1000-PCLU and 1.5–2.0% for PEG400-PCLU. Furthermore, the water absorption of the specimen increased with increasing the temperature of water bath, e.g. the water absorption of PEG400-PCLU increased to 5–10% in 50°C water bath. The absorbed water will swell the specimens and make the dimensions increase. The water absorption can result in a maximum dimensional in length extension about 1–3% for PTMG1000-PCLU, 10–25% for PEG1000-PCLU and less than 0.9–1.2% for PEG400-PCLU.

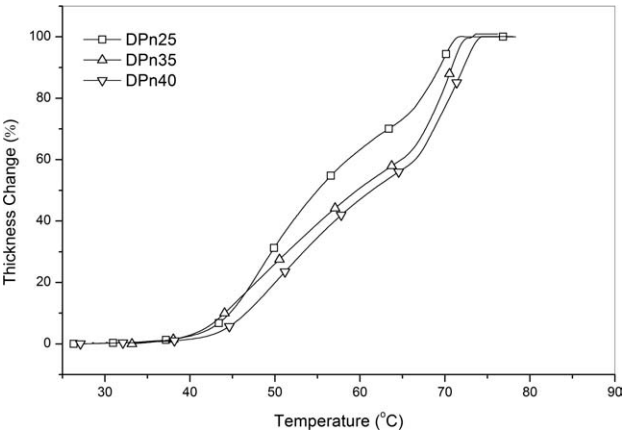

Figure 8. Typical compressive deformation recovery curves of PTMG1000-PCLU.

The Recovery of Compressive Deformation

Figure 8 shows typical recovery curves of compressive deformation carried out by DMA instrument with penetrate mode. The recovery curves for the specimens of different PCL block $\overline{DPn}$ s show slightly different LRTs (41–44°C) and URTs (71–74°C). The corresponding results were summarized in Table III. Both the LRT and URT increased with increasing the PCL block $\overline{DPn}$. The variation of the LRT and URT is anticipated according to the effect of crystallinity, especially the perfectness degree of PCL block crystal, on the recovery properties. In contrast, the higher crystallinity or more perfectness degree resulted from the increased PCL block $\overline{DPn}$, the more crystal microdomains can maintain their original state and the less portion of crystal was destructed. Therefore, the deformed specimens will start to recover its original shape at relatively higher temperature, owing to the ability of the deformed microdomains to fix the temporary shape of the specimen. In contrast, the URT of the specimens was related, to a great extent, to the T_m of the products. The T_m and perfectness degree of the crystal increases with increasing the crystallizable molecular chain length.[39] Thus, the URT of the specimen increased with the increase of the PCL block $\overline{DPn}$.

Inflexion temperatures were also observed in the recovery curves, similar to that in tensile deformation recovery. However, the inflexion temperature of compressive deformation recovery shifted to higher temperature region (64–66°C), which is much higher than those of the tensile deformation recovery. This phenomenon can be elucidated by two aspects. When the deformation step is inspected again, it can be easily found that the degree of deformation in compressive test is much lower than that in tensile test. In high deformation range, the tensile test in our work, most of the crystal microdomains were deformed highly into fibriform or laminar state. Although in relative low deformation range, the compressive test, the crystal microdomains were not deformed so much. This suggested that the degree of the crystal microdomains maintaining their original state in compressive test was greater than that in tensile test. In

Table III. Compressive Recovery Results for PCLU with Different Polyether Diols and $\overline{DPn}$ s

Sample	[a]LRT (°C)	[a]URT (°C)	[b]T_{MCF} (°C)	[c]MRF ◇MPa◇	R_f' (%)	R_r' (%)
PTMG1000-DPn25	24	71.2	41.83	4.63	71.3	100
PTMG1000-DPn30	26	71.1	42.87	5.91	68.9	100
PTMG1000-DPn35	27	72.2	43.09	5.34	71.5	100
PTMG1000-DPn40	30	73.4	44.23	5.97	71.2	100
PEG1000-DPn20	28	66.0	42.25	4.47	73.1	92.1
PEG1000-DPn25	30	67.2	43.87	4.88	71.8	92.0
PEG1000-DPn30	32	68.9	46.09	5.32	77.2	92.3
PEG1000-DPn35	33	70.2	46.85	5.53	77.2	92.1
PEG1000-DPn40	35	71.1	48.92	6.02	77.9	92.5

[a]LRT and URT are lowest recovery temperature and upper recovery temperature at which shape recovery starts and ends, respectively. LRT and URT were determined by DMA, [b]The temperature at which the MRF is measured in the retract force curve, [c]MRF is maximum retract force.

turn, the resulted decrease amplitude in T_m is relatively small after compressive test. Another reason for the inflexion temperature shift to high temperature is that the compressive deformation recovery test was performed with a relatively higher heating rate (5°C/min). In contrast, the temperature was elevated step by step and the deformed specimen could stay at every temperature for a relatively long time during the tensile deformation recovery test.

Concerning the temporary shape fixity R_f' of the specimens in compressive recovery test, its variation is similar to that in tensile recovery test and the values are close to those in tensile recovery. However, the recovery ratio R_r' in compressive recovery can all approach a relatively high level and the specimens can almost completely recover their original dimensions. This phenomenon can be anticipated if the effect of water absorption on the shape recovery was taken into consideration. The compressive deformation recovery tests in air atmosphere without much moisture. That is, the specimen can recover its original shape freely without the swelling effect of the absorbed water.

Because the recovery properties are determined to a great extent by the nature and perfectness degree of the PCL block crystal and the crystalline properties is affected by the temperature, the recovery properties of the products should be influenced by the temperature at which the PCL block crystal microdomains are deformed. In consideration of this effect, the recovery properties of PTMG1000-PCLU of $\overline{DPn}$ 35 were investigated by deforming the specimens at different temperatures. The shape recovery curves are shown in Figure 9. As expected, the R_f'can be improved and almost increased to 100% when deformed at elevated temperatures. Because some of the PCL crystal microdomains were melted at higher temperatures, the molecular chain can develop deformation fully to adapt the applied force. Besides, results show that the higher deformation temperatures lead to higher LRTs and lower URTs. And the LRT increased to almost the same level, approximately 47°C. Thus, the recovery temperature region is narrower than that of deformed at 25°C. When the deformation temperature was much lower than the T_m of PCL block, the PCL crystal microdomains were deformed much greater than that in higher temperatures and the destruction to the PCL crystal was much serious. These aspects lead to a lower LRT for the specimen deformed at 25°C. In addition, to deform a specimen at lower temperature needs more energy, and may even destroy the structure of the hard microdomains and crystal microdomains.

The inflexion temperatures were also observed in the curves and almost at the same point. It seems that the recovery curves of different deformation temperatures are rotated round the same inflexion point. This means that the inflexion temperature is not determined by the deformation temperature but by the PCL block $\overline{DPn}$. Therefore, the deformation temperature should be properly chosen according to different purposes. If a narrower recovery temperature range is required, the deformation temperature should be usually chosen in the range of 35–55°C to deform the PCL microdomains properly but avoid the destruction of the structure. However, if a lower LRT is required, the deformation temperature should be chosen near room temperature to deform the PCL microdomains greatly.

The Model of Shape Memory Process

According to discussed above, there are many ordered crystal microdomains with different perfectness degree of crystal in the product. For the shape memory product realized by utilizing crystalline component as reversible phase, the crystal

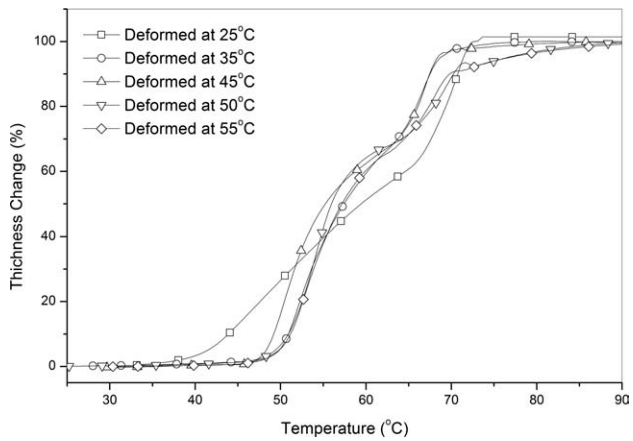

Figure 9. Compressive deformation recovery curves of PTMG1000-DPn35 deformed at different temperatures.

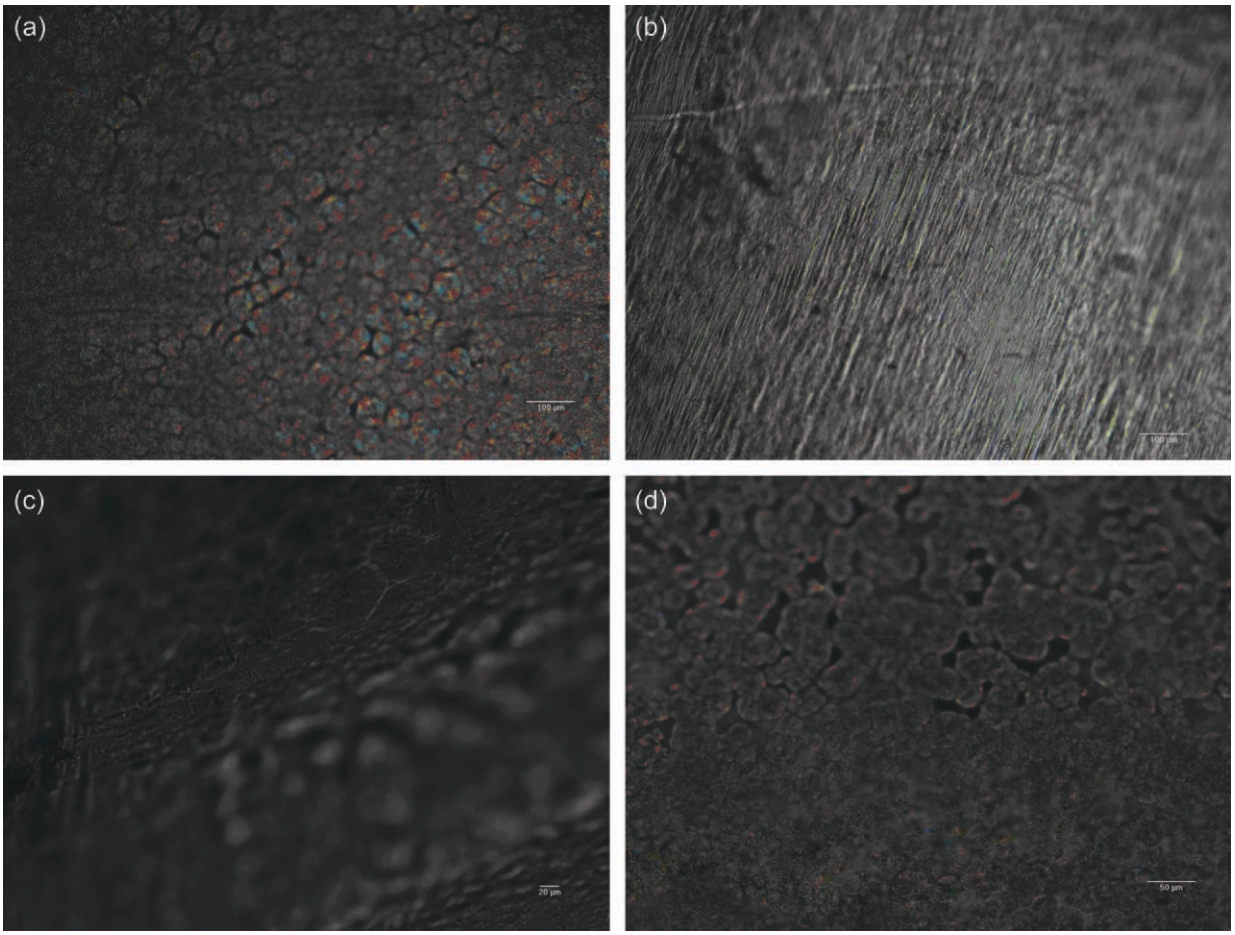

Figure 10. POM images of specimens (a) before deformation, (b) after deformation, (c) during recovery, and (d) after recovery and cooled to room temperature. [Color figure can be viewed in the online issue, which is available at wileyonlinelibrary.com.]

microdomains play a vital important role in the process of shape recovery. When deformed, some of the crystal microdomains were deformed from spherular to fibriform or laminar state (as shown in Figure 10(b)), and some were destructed to be amorphous state. DSC measurements show that the crystallinity of samples after deformation decreased by 4.2–8.7% compared with samples before deformation. With the development of the deformation of crystal, the optical status of specimens varied from opaque to translucent or transparent.

According to the deformation process described above, a modified model was postulated to elucidate the shape recovery process (as shown in Scheme 1). During the recovery of the deformed specimen on heating, the deformed crystal microdomains have at least two effects on the shape recovery of the sample. First, the deformed but not destructed parts will recover their original microdomain shape, which, to a great extent, drives the recovery of the whole bulk specimen. Second, in the primary stage, as the temperature is elevated but below the T_m of the most perfect PCL block crystal, the deformed more perfect PCL block crystal microdomains act as physical cross links to help the deformed specimen to recover original dimension as well as the cross links set by the polyurethane microphase separation.[4,16] As the temperature is continued to be elevated to approach and exceed the T_m of the most perfect PCL block crystal, the cross links set by crystal microdomains is disassociated and disappears gradually due to the melting of all the PCL block crystal. In the second stage, the deformed specimen recovers its original shape only driven by the cross links set by the polyurethane microphase separation. The model can be visualized by the POM images of crystal microdomains during the tensile deformation recovery cycle (Figure 10).

These two stages of recovery process can be verified by the DSC analyses, for there is a crystalline melting region (the region between the two parallel dash lines in Figure 2) before the melting peak, the melting of which resulted in the first stage recovery Another evidence for the two stages of recovery process is that the retract force developed with two stages, which will be discussed in the following sections. In general, the retract force increased and reached its maximum below the T_m of PCL block crystal. And the retract force decreased when the T_m of PCL block crystal approached, but the deformed specimen can still continued to restore its original shape. That is, below the T_m of PCL block crystal, the retract force is determined not only by the cross links set by the polyurethane microphase separation but also by the cross links set by PCL block crystal microdomains. Above the T_m of PCL block crystal, the retract force is determined only by the former.

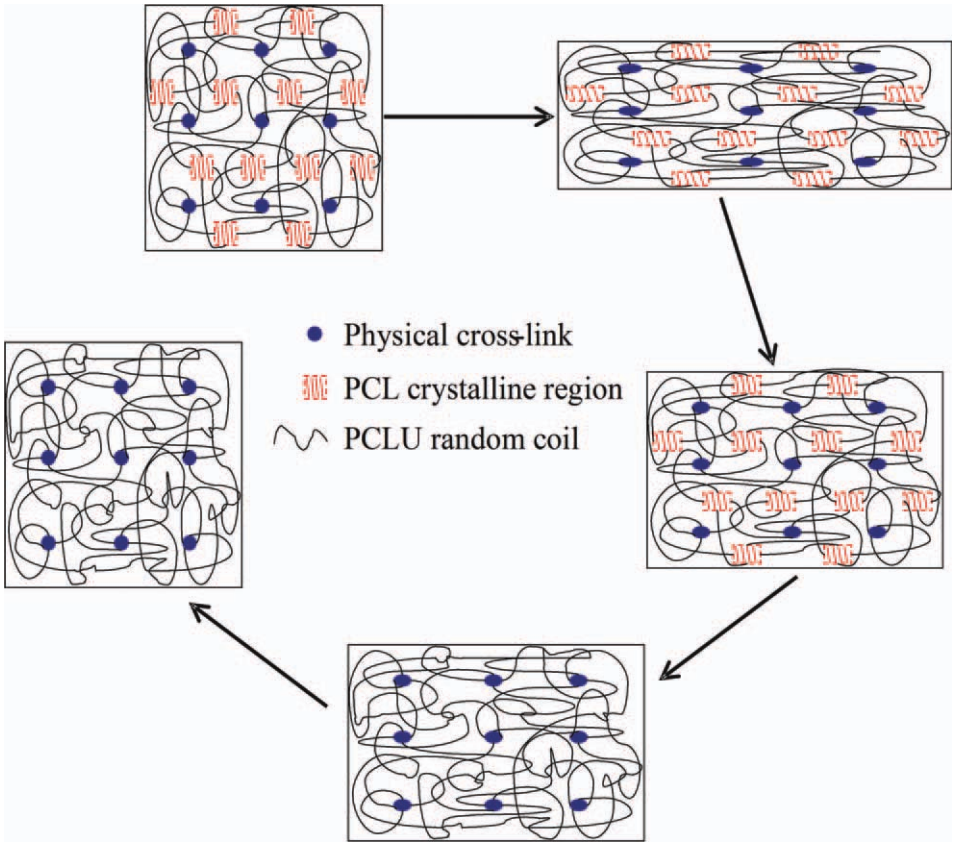

Scheme 1. Illustration of the shape memory mechanism of PCLU. [Color figure can be viewed in the online issue, which is available at wileyonlinelibrary.com.]

CONCLUSIONS

The T_m, T_c, and X_c of PCLU synthesized via a novel route of reactive extrusion in a mass scale are dependent on the PCL block $\overline{DPn}$ and original polyether type. The effect of the restriction of polyether block on the crystallization of the PCL block decreased with the increase of the PCL block $\overline{DPn}$. The retract force increased with increasing the temperature and reached its maximum in the temperature range of 45–55°C. The retract force of PCLU was determined by the cross links set by the PCL block crystal microdomains and the polyurethane microphase separation. The maximum retract force of PCLUs is 6–7 MPa which is as high as that of PLAUs.

The influences of PCL block $\overline{DPn}$ on the tensile and compressive deformation recovery properties are similar for PCLUs originated from different polyether diols. The two stages in the recovery process were distinguished by the inflexion temperature, approximately 43–48°C in tensile deformation recovery and shift to 64–66°C in compressive deformation recovery, which determined not by the deformation temperature but by the PCL block $\overline{DPn}$. In tensile deformation recovery, the R_f of products was around 60–70% without significant differences among various products and the R_r was greatly affected by absorbed water and increased with increasing the PCL block $\overline{DPn}$. The R_f and R_r of 200% prefixed elongation are more than those of 300%. Although in compressive deformation recovery, the R_r' can reach almost 100% by choosing deformation temperature. Besides, the higher deformation temperatures lead to higher LRTs and lower URTs.

In addition, POM results exhibit visually the changes of the PCL crystal microdomains during the deformation–recovery cycle. It was verified to be quite good for the postulated modified model to elucidate the development of retract force and recovery of dimensions.

ACKNOWLEDGMENTS

The authors thank Shanghai International Science and Technology Cooperation Funding (grant number 06SR07103), Shanghai Leading Academic Discipline Project (grant number B502), and Shanghai Key Laboratory Project (grant number 08DZ2230500).

REFERENCES

1. Lendlein, A.; Kelch, S. *Angew. Chem. Int. Ed.* **2002,** *41*, 2034.
2. Langer, R.; Tirrell, D. A. *Nature* **2004,** *428*, 487.
3. Guan, Y.; Cao, Y. P.; Peng, Y. X.; Xu, J.; Chen, A. S. C. *Chem. Commun.* **2001,** *(17)*, 1694.
4. Kim, B. K.; Shin, Y. J.; Cho, S. M.; Jeong, H. M. *J. Polym. Sci. Part B: Polym. Phys.* **2000,** *38*, 2652.
5. Kim, B. K.; Lee, S. Y. *Polymer* **1996,** *37*, 5781.

6. Li, F. K.; Chen, Y.; Zhu, W.; Zhang, X.; Xu, M. *Polymer* **1998,** *39*, 6929.
7. Li, F. K.; Zhang, X.; Hou, J.; Xu, M.; Luo, X. L.; Ma, D. Z.; Kim, B. K. *J. Appl. Polym. Sci.* **1997,** *64*, 1511.
8. Ma, D. Z.; Wang, M. T.; Wang, M. Z.; Zhang, X. Y.; Luo, X. L. *J. Appl. Polym. Sci.* **1998,** *69*, 947.
9. Luo, X. L.; Zhang, X. Y.; Wang, M. T.; Ma, D. Z.; Xu, M.; Li, F. K. *J. Appl. Polym. Sci.* **1997,** *64*, 2433.
10. Wang, M. T.; Luo, X. L.; Zhang, X. Y.; Ma, D. Z. *Polym. Adv. Technol.* **1997,** *8*, 136.
11. Lee, B. S.; Chun, B. C.; Chung, Y. C.; Sul, K. I. Cho, J. W. *Macromolecules* **2001,** *34*, 6431.
12. Liu, C. D.; Chun, S. B.; Mather, P. T.; Zheng, L.; Haley, E. H.; Coughlin, E. B. *Macromolecules* **2002,** *35*, 9868.
13. Rousseau, I. A.; Mather, P. T. *J. Am. Chem. Soc.* **2003,** *125*, 15300.
14. Lin, J. R.; Chen, L. W. *J. Appl. Polym. Sci.* **1998,** *69*, 1563.
15. Lin, J. R.; Chen, L. W. *J. Appl. Polym. Sci.* **1998,** *69*, 1575.
16. Liu, G. Q.; Ding, X. B.; Cao, Y. P.; Zheng, Z. H.; Peng, Y. X. *Macromolecules* **2004,** *37*, 2228.
17. Lendlein, A.; Langer, R. *Science* **2002,** *296*, 1673.
18. Tobushi, H.; Hara, H.; Yamada, E.; Hayashi, S. *Smart Mater. Struct.* **1996,** *5*, 483.
19. Ding, X. M.; Hu, J. L.; Tao, X. M. *Text. Res. J.* **2004,** *74*, 39.
20. Ji, F. L.; Hu, J. L.; Li, T. C.; Wong, Y. W. *Polymer* **2007,** *48*, 5133.
21. Bogart, V.; John, W. C.; Gibson, P. E.; Cooper, S. L. *J. Polym. Sci. Polym. Phys. Ed.* **1983,** *21*, 65.
22. Chu, B.; Gao, T.; Li, Y.; Wang, J.; Desper, C. R.; Catherine, A. B. *Macromolecules* **1992,** *25*, 5724.
23. Koberstein, J. T.; Galambos, A. F.; Leung, L. M. *Macromolecules* **1992,** *25*, 6195.
24. Velankar, S.; Cooper, S. L. *Macromolecules* **2000,** *33*, 382.
25. Ryan, A. J.; Willkomm, W. R.; Bergstrom, T. B.; Macosko, C. W.; Koberstein, J. T.; Yu, C. C.; Russell, T. P. *Macromolecules* **1991,** *24*, 2883.
26. Sonnenschein, M. F.; Lysenko, Z.; Brune, D. A.; Wendt, B. L.; Schrock, A. K. *Polymer* **2005,** *46*, 10158.
27. Heijkants, R. G. J. C.; Schwab, L. W.; van Calck, R. V.; de Groot, J. H.; Pennings, A. J.; Schouten, A. J. *Polymer* **2005,** *46*, 8981.
28. Korley, L. T. J.; Pate, B. D.; Thomas, E. L.; Hammond, P. T. *Polymer* **2006,** *47*, 3073.
29. Hu, J. L.; Ji, F. L.; Wong, Y. W. *Polym. Int.* **2005,** *54*, 600.
30. Laity, P. R.; Taylor, J. E.; Wong, S. S.; Khunkamchoo, P.; Norrisb, K.; Cable, M.; Andrews, G. T.; Johnson, A. F.; Cameron, R. E. *Polymer* **2004,** *45*, 7273.
31. Blundell, D. J.; Eeckhaut, G.; Fuller, W.; Mahendrasingam, A.; Martin, C. *Polymer* **2002,** *43*, 5197.
32. Yi, J.; Boyce, M. C.; Lee, G. F.; Balizer, E. *Polymer* **2006,** *47*, 319.
33. Christenson, E. M.; Anderson, J. M.; Hiltner, A.; Baer, E. *Polymer* **2005,** *46*, 11744.
34. Weng, S. G.; Xia, Z. A.; Chen, J. D.; Gong, L. L.; Xu, R. J. *J. Appl. Polym. Sci.* **2012,** *124*, 3765.
35. Crescenzi, V.; Manzini, G.; Calzolari, G.; Borri, C. *Eur. Polym. J.* **1972,** *8*, 449.
36. He, C. L.; Sun, J. R.; Deng, C.; Zhao, T.; Deng, M. X.; Chen, X. S.; Jing, X. B. *Biomacromolecules* **2004,** *5*, 2042.
37. Gan, Z. H.; Jiang, B. Z.; Zhang, J. *J. Appl. Polym. Sci.* **1996,** *59*, 961.
38. Shiomi, T.; Imai, K.; Takenaka, K.; Takeshita, H.; Hayashi, H.; Tezuka, Y. *Polymer* **2001,** *42*, 3233.
39. Flory, P. J. *Trans. Faraday Soc.* **1955,** *51*, 848.
40. Ping, P.; Wang, W. S.; Chen, X. S.; Jing, X. B. *Biomacromolecules* **2005,** *6*, 587.
41. Ping, P.; Wang, W. S.; Zhang, P. B.; Chen, X. S.; Jing, X. B. *Chem. J. Chin. Univ.* **2007,** *8*, 371.